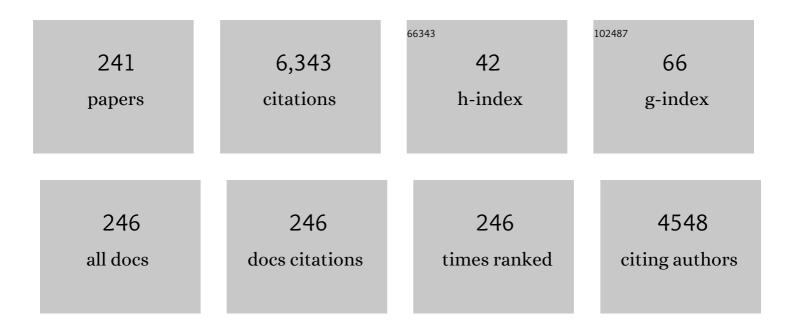
## Inocencio Rafael Martin

List of Publications by Year in descending order

Source: https://exaly.com/author-pdf/213295/publications.pdf Version: 2024-02-01



#	Article	IF	CITATIONS
1	Role of the host matrix on the thermal sensitivity of Er3+ luminescence in optical temperature sensors. Sensors and Actuators B: Chemical, 2012, 174, 176-186.	7.8	168
2	In Vivo Subcutaneous Thermal Video Recording by Supersensitive Infrared Nanothermometers. Advanced Functional Materials, 2017, 27, 1702249.	14.9	159
3	Dopant distribution in a Tm3+–Yb3+ codoped silica based glass ceramic: An infrared-laser induced upconversion study. Journal of Chemical Physics, 2004, 120, 6180-6190.	3.0	157
4	Effects of Er3+ concentration on thermal sensitivity in optical temperature fluorotellurite glass sensors. Sensors and Actuators B: Chemical, 2013, 176, 1167-1175.	7.8	137
5	High‣ensitivity Fluorescence Lifetime Thermal Sensing Based on CdTe Quantum Dots. Small, 2012, 8, 2652-2658.	10.0	130
6	Luminescent Nanothermometer Operating at Very High Temperature—Sensing up to 1000 K with Upconverting Nanoparticles (Yb <sup>3+</sup> /Tm <sup>3+</sup> ). ACS Applied Materials & Interfaces, 2020, 12, 43933-43941.	8.0	130
7	Comparison of the sensitivity as optical temperature sensor of nano-perovskite doped with Nd3+ ions in the first and second biological windows. Sensors and Actuators B: Chemical, 2018, 255, 970-976.	7.8	110
8	On the local structure of Eu3+ ions in oxyfluoride glasses. Comparison with fluoride and oxide glasses. Journal of Chemical Physics, 2001, 115, 10935-10944.	3.0	109
9	Optical characterization of Er3+-doped zinc fluorophosphate glasses for optical temperature sensors. Sensors and Actuators B: Chemical, 2013, 186, 156-164.	7.8	107
10	Characterization of Er3+ and Nd3+ doped Strontium Barium Niobate glass ceramic as temperature sensors. Optical Materials, 2011, 33, 742-745.	3.6	104
11	Neodymium-doped nanoparticles for infrared fluorescence bioimaging: The role of the host. Journal of Applied Physics, 2015, 118, .	2.5	102
12	Optical Vacuum Sensor Based on Lanthanide Upconversion—Luminescence Thermometry as a Tool for Ultralow Pressure Sensing. Advanced Materials Technologies, 2020, 5, 1901091.	5.8	102
13	Upconversion mechanisms in rare-earth doped glasses to improve the efficiency of silicon solar cells. Solar Energy Materials and Solar Cells, 2011, 95, 1671-1677.	6.2	99
14	Optical spectroscopy analysis of the Eu3+ ions local structure in calcium diborate glasses. Journal of Non-Crystalline Solids, 2003, 319, 200-216.	3.1	91
15	Upconverting lanthanide doped fluoride NaLuF4:Yb3+-Er3+-Ho3+ - optical sensor for multi-range fluorescence intensity ratio (FIR) thermometry in visible and NIR regions. Journal of Luminescence, 2018, 201, 104-109.	3.1	91
16	Analysis of Er3+ and Ho3+ codoped fluoroindate glasses as wide range temperature sensor. Materials Research Bulletin, 2011, 46, 1051-1054.	5.2	90
17	Energy transfer with migration. Generalization of the Yokota–Tanimoto model for any kind of multipole interaction. Journal of Chemical Physics, 1999, 111, 1191-1194.	3.0	87
18	Optical properties of Nd3+ ions in oxyfluoride glasses and glass ceramics comparing different preparation methods. Journal of Applied Physics, 2004, 95, 5271-5279.	2.5	83

#	Article	IF	CITATIONS
19	Optical properties of Er3+ ions in transparent glass ceramics. Journal of Alloys and Compounds, 2001, 323-324, 753-758.	5.5	81
20	Relevance of radiative transfer processes on Nd3+ doped phosphate glasses for temperature sensing by means of the fluorescence intensity ratio technique. Sensors and Actuators B: Chemical, 2014, 195, 324-331.	7.8	80
21	Sr <sub>2</sub> LuF <sub>7</sub> :Yb <sup>3+</sup> –Ho <sup>3+</sup> –Er <sup>3+</sup> Upconverting Nanoparticles as Luminescent Thermometers in the First, Second, and Third Biological Windows. ACS Applied Nano Materials, 2020, 3, 6406-6415.	5.0	80
22	Cooperative energy transfer in Yb3+–Tb3+ codoped silica sol-gel glasses. Journal of Applied Physics, 2001, 89, 2520-2524.	2.5	78
23	Optical properties and cross relaxation among Sm3+ ions in fluorzincate glasses. Journal of Luminescence, 1992, 54, 231-236.	3.1	73
24	Locating median cycles in networks. European Journal of Operational Research, 2005, 160, 457-470.	5.7	73
25	Variable neighborhood tabu search and its application to the median cycle problem. European Journal of Operational Research, 2003, 151, 365-378.	5.7	70
26	Ultraviolet and white photon avalanche upconversion in Ho3+-doped nanophase glass ceramics. Applied Physics Letters, 2005, 86, 051106.	3.3	70
27	Er3+–Yb3+ codoped phosphate glasses used for an efficient 1.5μ m broadband gain medium. Optical Materials, 2012, 34, 1235-1240.	3.6	69
28	Praseodymium doped YF3:Pr3+ nanoparticles as optical thermometer based on luminescence intensity ratio (LIR) – Studies in visible and NIR range. Journal of Luminescence, 2019, 214, 116571.	3.1	65
29	Increase of the 800 nm excited Tm3+ blue upconversion emission in fluoroindate glasses by codoping with Yb3+ ions. Optical Materials, 2003, 22, 327-333.	3.6	62
30	Rare earths in nanocrystalline glass–ceramics. Optical Materials, 2005, 27, 1762-1770.	3.6	62
31	Random laser in biological tissues impregnated with a fluorescent anticancer drug. Laser Physics Letters, 2015, 12, 045805.	1.4	57
32	Optical pressure sensing in vacuum and high-pressure ranges using lanthanide-based luminescent thermometer–manometer. Journal of Materials Chemistry C, 2021, 9, 4643-4651.	5.5	56
33	Role of the Eu3+ ions in the formation of transparent oxyfluoride glass ceramics. Journal of Applied Physics, 2001, 89, 5307-5310.	2.5	55
34	Site selective study of Eu3+-doped transparent oxyfluoride glass ceramics. Journal of Applied Physics, 2003, 94, 2295-2301.	2.5	55
35	2CaO·Al 2 O 3 :Er 3+ glass: An efficient optical temperature sensor. Journal of Luminescence, 2016, 179, 272-279.	3.1	54
36	Upconversion dynamics in Yb3+–Ho3+ doped fluoroindate glasses. Journal of Alloys and Compounds, 1998, 275-277, 345-348.	5.5	50

#	Article	IF	CITATIONS
37	Infrared-laser induced photon avalanche upconversion in Ho3+–Yb3+ codoped fluoroindate glasses. Journal of Applied Physics, 2004, 95, 2957-2962.	2.5	50
38	Er3+-doped tellurite glasses for enhancing a solar cell photocurrent through photon upconversion upon 1500Anm excitation. Materials Chemistry and Physics, 2017, 199, 67-72.	4.0	49
39	Synthesis and characterization of SrSnO <sub>3</sub> doped with Er <sup>3+</sup> for up-conversion luminescence temperature sensors. RSC Advances, 2017, 7, 46796-46802.	3.6	49
40	Optical intensities of Pr3+ ions in transparent oxyfluoride glass and glass–ceramic. Applications of the standard and modified Judd–Ofelt theories. Journal of Alloys and Compounds, 2004, 380, 167-172.	5.5	48
41	Pressure-induced energy transfer processes betweenSm3+ions in lithium fluoroborate glasses. Physical Review B, 2002, 66, .	3.2	45
42	Experimental enhancement of the photocurrent in a solar cell using upconversion process in fluoroindate glasses exciting at 1480nm. Solar Energy Materials and Solar Cells, 2013, 116, 171-175.	6.2	44
43	A phase transition in the novel three-dimensional compound [Eu2(mal)3(H2O)6] (H2mal = malonic acid). Dalton Transactions RSC, 2002, , 3462-3470.	2.3	40
44	Infrared-to-visible photon avalanche upconversion dynamics in Ho3+-doped fluorozirconate glasses at room temperature. Optical Materials, 2005, 27, 1754-1761.	3.6	40
45	Near-infrared and upconversion luminescence of Tm3+ and Tm3+/Yb3+-doped oxyfluorosilicate glasses. Journal of Non-Crystalline Solids, 2019, 507, 1-10.	3.1	40
46	Judd-Ofelt parameters of RE3+-doped fluorotellurite glass (RE3+= Pr3+, Nd3+, Sm3+, Tb3+, Dy3+, Ho3+,) Tj ETQ	<u>)</u> q0 0 0 rgl	BT /Overlock 1 40
47	Whispering gallery modes in a glass microsphere as a function of temperature. Optics Express, 2011, 19, 25792.	3.4	39
48	Structure and NIR-luminescence of ytterbium(iii) beta-diketonate complexes with 5-nitro-1,10-phenanthroline ancillary ligand: assessment of chain length and fluorination impact. Dalton Transactions, 2013, 42, 13516.	3.3	38
49	Liquid whispering-gallery-mode resonator as a humidity sensor. Optics Express, 2017, 25, 1165.	3.4	38
50	Inert Shell Effect on the Quantum Yield of Neodymium-Doped Near-Infrared Nanoparticles: The Necessary Shield in an Aqueous Dispersion. Nano Letters, 2020, 20, 7648-7654.	9.1	37
51	Nonlinear Optical Thermometry—A Novel Temperature Sensing Strategy via Second Harmonic Generation (SHG) and Upconversion Luminescence in BaTiO <sub>3</sub> :Ho <sup>3+</sup> ,Yb <sup>3+</sup> Perovskite. Advanced Optical Materials, 2021, 9, 2100386.	7.3	37
52	Infrared, blue and ultraviolet upconversion emissions in Yb3+–Tm3+-doped fluoroindate glasses. Spectrochimica Acta - Part A: Molecular and Biomolecular Spectroscopy, 1999, 55, 941-945.	3.9	36
53	Spectroscopy and radiation trapping of Yb3+ ions in lead phosphate glasses. Journal of Quantitative Spectroscopy and Radiative Transfer, 2014, 140, 37-47.	2.3	36
54	Structure, morphology and optical characterization of Dy 3+ -doped BaYF 5 nanocrystals for warm	3.6	36

Structure, morphology and optical characterization of Dy 3+ -dop white light emitting devices. Optical Materials, 2017, 70, 16-24. 54

#	Article	IF	CITATIONS
55	Spectroscopy of rare earth ions in fluoride glasses for laser applications. Optical Materials, 1999, 13, 1-7.	3.6	35
56	Novel erbium(iii) complexes with 2,6-dimethyl-3,5-heptanedione and different N,N-donor ligands for ormosil and PMMA matrices doping. Journal of Materials Chemistry C, 2013, 1, 5701.	5.5	35
57	Supersensitive Ratiometric Thermometry and Manometry Based on Dualâ€Emitting Centers in Eu <sup>2+</sup> /Sm <sup>2+</sup> â€Doped Strontium Tetraborate Phosphors. Advanced Optical Materials, 2022, 10, .	7.3	35
58	Chemical pressure effects on the spectroscopic properties of Nd^3+-doped gallium nano-garnets. Optical Materials Express, 2015, 5, 1661.	3.0	34
59	Optical thermometry based on upconversion emissions in Na3Gd (VO4)2: Yb3+-Er3+/Ho3+ micro crystals. Journal of Alloys and Compounds, 2022, 891, 161993.	5.5	34
60	Site selective study in Eu3+-doped fluorozirconate glasses and glass-ceramics. Journal of Luminescence, 1997, 72-74, 437-438.	3.1	33
61	Room temperature photon avalanche upconversion in Tm3+-doped fluoroindate glasses. Journal of Physics Condensed Matter, 2000, 12, 1507-1516.	1.8	33
62	Locating a cycle in a transportation or a telecommunications network. Networks, 2007, 50, 92-108.	2.7	33
63	Cross-relaxation for Tm3+ ions in indium-based glasses. Journal of Non-Crystalline Solids, 1993, 161, 294-296.	3.1	31
64	Ultraviolet- and Near-Infrared-Excitable LaPO <sub>4</sub> :Yb <sup>3+</sup> /Tm <sup>3+</sup> /Ln <sup>3+</sup> (Ln = Eu, Tb) Nanoparticles for Luminescent Fibers and Optical Thermometers. ACS Applied Nano Materials, 2020, 3, 6541-6551.	5.0	31
65	Temperature dependence of Nd3+↔Yb3+ energy transfer in the YAl3(BO3)4 nonlinear laser crystal. Journal of Applied Physics, 2005, 97, 093510.	2.5	30
66	Optical properties of Er3+-doped strontium barium niobate nanocrystals obtained by thermal treatment in glass. Journal of Luminescence, 2008, 128, 908-910.	3.1	28
67	Stark level structure and oscillator strengths of Nd3+ ion in different fluoride single crystals. Journal of Alloys and Compounds, 2001, 323-324, 763-767.	5.5	27
68	Active layer solution-processed NIR-OLEDs based on ternary erbium( <scp>iii</scp> ) complexes with 1,1,1-trifluoro-2,4-pentanedione and different N,N-donors. Dalton Transactions, 2014, 43, 18087-18096.	3.3	27
69	Spectroscopic studies on Yb 3+ -doped tungsten-tellurite glasses for laser applications. Journal of Non-Crystalline Solids, 2018, 479, 9-15.	3.1	27
70	Whispering-gallery modes in glass microspheres: optimization of pumping in a modified confocal microscope. Optics Letters, 2011, 36, 615.	3.3	26
71	Novel perovskite ceramics for chemical looping combustion application. Journal of CO2 Utilization, 2016, 13, 95-104.	6.8	25
72	Structural properties, Judd–Ofelt calculations, and near infrared to visible photon up-conversion in Er <sup>3+</sup> /Yb <sup>3+</sup> doped BaTiO <sub>3</sub> phosphors under excitation at 1500 nm. RSC Advances, 2017, 7, 10529-10538.	3.6	25

#	Article	IF	CITATIONS
73	Lanthanide-doped Y3Ga5O12 garnets for nanoheating and nanothermometry in the first biological window. Optical Materials, 2018, 84, 46-51.	3.6	25
74	Luminescent Nd <sup>3+</sup> â€Based Microresonators Working as Optical Vacuum Sensors. Advanced Optical Materials, 2020, 8, 2000678.	7.3	25
75	Ultraviolet and visible upconversion luminescence in Nd3+-doped oxyfluoride glasses and glass ceramics obtained by different preparation methods. Journal of Applied Physics, 2006, 99, 113510.	2.5	24
76	Optical gain in dye-impregnated oxidized porous silicon waveguides. Applied Physics Letters, 2006, 89, 011107.	3.3	24
77	Crystallization of nano calcium fluoride in CaF2–Al2O3–SiO2 system. Solid State Sciences, 2013, 17, 76-82.	3.2	24
78	Optimizing white light luminescence in Dy3+-doped Lu3Ga5O12 nano-garnets. Journal of Applied Physics, 2014, 116, .	2.5	24
79	Analysis of the upconversion process in Tm3+ doped glasses for enhancement of the photocurrent in silicon solar cells. Solar Energy Materials and Solar Cells, 2016, 144, 29-32.	6.2	24
80	Er3+/Ho3+ codoped nanogarnet as an optical FIR based thermometer for a wide range of high and low temperatures. Journal of Alloys and Compounds, 2020, 847, 156541.	5.5	24
81	A novel optical thermometry strategy based on emission of Tm <sup>3+</sup> /Yb <sup>3+</sup> codoped Na <sub>3</sub> GdV <sub>2</sub> O <sub>8</sub> phosphors. Dalton Transactions, 2022, 51, 5108-5117.	3.3	24
82	Upconversion dynamics in Er3+-doped fluoroindate glasses. Spectrochimica Acta - Part A: Molecular and Biomolecular Spectroscopy, 1999, 55, 935-940.	3.9	23
83	Dopant partitioning influence on the near-infrared emissions of Tm3+ in oxyfluoride glass ceramics. Journal of Applied Physics, 2006, 99, 053103.	2.5	23
84	Temperature dependence of Nd3+→Yb3+ energy transfer processes in co-doped oxyfluoride glass ceramics. Journal of Non-Crystalline Solids, 2007, 353, 1951-1955.	3.1	23
85	Quantum cutting and near-infrared emissions in Ho3+/Yb3+ codoped transparent glass-ceramics. Journal of Luminescence, 2020, 226, 117424.	3.1	23
86	Enhanced red up-conversion emission in Er3+/Yb3+ co-doped SrSnO3 for optical temperature sensing based on thermally and non-thermally coupled levels. Journal of Luminescence, 2022, 244, 118687.	3.1	23
87	Effect of pH on the optical and structural properties of HfO2:Ln3+, synthesized by hydrothermal route. Journal of Luminescence, 2016, 175, 243-248.	3.1	22
88	Yttrium orthoaluminate nanoperovskite doped with Tm^3+ ions as upconversion optical temperature sensor in the near-infrared region. Optics Express, 2017, 25, 27845.	3.4	22
89	Optical properties and upconversion in Yb3+—Tm3+co-doped oxyfluoride glasses and glass ceramics. Molecular Physics, 2003, 101, 1057-1065.	1.7	21
90	Effect of pressure on the luminescence properties of Nd3+ doped SrWO4 laser crystal. Journal of Alloys and Compounds, 2008, 451, 212-214.	5.5	21

INOCENCIO RAFAEL MARTIN

#	Article	IF	CITATIONS
91	An erbium(III)-based NIR emitter with a highly conjugated $\hat{I}^2$ -diketonate for blue-region sensitization. Journal of Alloys and Compounds, 2015, 619, 553-559.	5.5	21
92	High pressure luminescence of Nd3+ in YAlO3 perovskite nanocrystals: A crystal-field analysis. Journal of Chemical Physics, 2018, 148, 044201.	3.0	21
93	Transfer and back transfer processes in Yb3+–Er3+ codoped fluoroindate glasses. Journal of Applied Physics, 1999, 86, 935-939.	2.5	20
94	Improved Cooperative Emission in Ytterbiumâ€Doped Oxyfluoride Glass eramics Containing <scp><scp>CaF</scp></scp> <sub>2</sub> Nanocrystals. Journal of the American Ceramic Society, 2012, 95, 3827-3833.	3.8	20
95	Energy transfer between Eu3+ions in calcium diborate glasses. Journal of Physics Condensed Matter, 1999, 11, 8739-8747.	1.8	19
96	Preparation and optical spectroscopy of Eu3+-doped GaN luminescent semiconductor from freeze-dried precursors. Journal of Solid State Chemistry, 2004, 177, 4213-4220.	2.9	19
97	Local devitrification of Dy3+ doped Ba2TiSi2O8 glass by laser irradiation. Optical Materials, 2010, 33, 186-190.	3.6	19
98	Synthesis, characterization and optical spectroscopy of Eu3+ doped titanate nanotubes. Journal of Luminescence, 2011, 131, 2473-2477.	3.1	19
99	Upconversion emission of ZrO2 nanoparticles doped with erbium (Er3+) and ytterbium (Yb3+), synthesized by hydrothermal route. Ceramics International, 2018, 44, 154-157.	4.8	19
100	CdVO4:Er3+/Yb3+ nanocrystalline powder as fluorescence temperature sensor. Application to monitor the temperature of an electrical component. Sensors and Actuators A: Physical, 2019, 299, 111628.	4.1	19
101	Room-temperature photon avalanche upconversion inTm3+:Y2O3crystals. Physical Review B, 1999, 60, 7252-7257.	3.2	18
102	Room temperature photon avalanche up-conversion in Ho3+ doped fluoroindate glasses under excitation at 747 nm. Optical Materials, 2004, 25, 209-213.	3.6	18
103	High pressure tuning of whispering gallery mode resonances in a neodymium-doped glass microsphere. Journal of the Optical Society of America B: Optical Physics, 2013, 30, 3254.	2.1	18
104	Carbon dots as temperature nanosensors in the physiological range. Journal of Luminescence, 2018, 196, 313-315.	3.1	18
105	Theoretical analysis of the photon avalanche dynamics in Ho3+-Yb3+ codoped systems under near-infrared excitation. Physical Review B, 2005, 71, .	3.2	17
106	Photon avalanche upconversion in Ho3+–Yb3+ co-doped transparent oxyfluoride glass–ceramics. Chemical Physics Letters, 2014, 600, 34-37.	2.6	17
107	Highly fluorinated erbium(III) complexes for emission in the C-band. Journal of Photochemistry and Photobiology A: Chemistry, 2014, 292, 16-25.	3.9	17
108	Structure, luminescence and magnetic properties of an erbium(iii) β-diketonate homodinuclear complex. New Journal of Chemistry, 2016, 40, 8251-8261.	2.8	17

#	Article	IF	CITATIONS
109	Amorphous glass-perovskite composite as solid electrolyte for lithium-ion battery. Materials Letters, 2019, 254, 294-296.	2.6	17
110	Luminescence whispering gallery modes in Ho3+ doped microresonator glasses for temperature sensing. Journal of Alloys and Compounds, 2019, 777, 198-203.	5.5	17
111	Optical properties of transparent Dy3+ doped Ba2TiSi2O8 glass ceramic. Optical Materials, 2011, 33, 738-741.	3.6	16
112	Time-resolved fluorescence line narrowing inYb3+-doped fluoroindate glasses. Physical Review B, 1998, 57, 3396-3401.	3.2	15
113	Fano antiresonances of Cr3+ in alkaline disilicate glasses. Spectrochimica Acta - Part A: Molecular and Biomolecular Spectroscopy, 1999, 55, 1319-1322.	3.9	15
114	Pump and probe measurements of optical amplification at 584nm in dysprosium doped lithium niobate crystal. Optical Materials, 2010, 33, 196-199.	3.6	15
115	Upconversion emission obtained in Yb^3+-Er^3+ doped fluoroindate glasses using silica microspheres as focusing lens. Optics Express, 2013, 21, 10667.	3.4	15
116	Increase of the blue upconversion emission in YAC:Tm3+ nanopowders by codoping with Yb3+ ions. Journal of Luminescence, 2008, 128, 924-926.	3.1	14
117	Infraredâ€ŧoâ€Visible Light Conversion in Er <sup>3+</sup> –Yb <sup>3+</sup> :Lu <sub>3</sub> Ga <sub>5</sub> O <sub>12</sub> Nanogarnets. ChemPhysChem, 2015, 16, 3928-3936.	2.1	14
118	Synthesis, characterization and spectroscopic properties of a new Nd 3+ -doped Co-picromerite-type Tutton salt. Journal of Luminescence, 2016, 177, 93-98.	3.1	14
119	Analysis of the upconversion emission of yttrium orthoaluminate nano-perovskite co-doped with Er3+/Yb3+ ions for thermal sensing applications. Journal of Luminescence, 2018, 202, 316-321.	3.1	14
120	Whispering gallery modes in a holmium doped glass microsphere: Temperature sensor in the second biological window. Optical Materials, 2018, 83, 207-211.	3.6	14
121	Near-infrared to visible upconversion and second harmonic generation in BaTiO3:Ho3+ and BaTiO3:Ho3+/Yb3+ phosphors. Journal of Alloys and Compounds, 2019, 806, 1146-1152.	5.5	14
122	Luminescent-plasmonic core–shell microspheres, doped with Nd3+ and modified with gold nanoparticles, exhibiting whispering gallery modes and SERS activity. Journal of Rare Earths, 2019, 37, 1152-1156.	4.8	14
123	Boltzmann vs. non-Boltzmann (non-linear) thermometry - Yb3+-Er3+ activated dual-mode thermometer and phase transition sensor via second harmonic generation. Journal of Alloys and Compounds, 2022, 906, 164329.	5.5	14
124	Analysis of the Eu3+emission in a SrWO4laser matrix under pressure. High Pressure Research, 2006, 26, 355-359.	1.2	13
125	Laser irradiation in Nd3+ doped strontium barium niobate glass. Journal of Applied Physics, 2008, 104, 013112.	2.5	13
126	Effect of alumina content and heat treatment on microstructure and upconversion emission of Er3+ ions in oxyfluoride glass-ceramics. Journal of Rare Earths, 2012, 30, 1228-1234.	4.8	13

#	Article	IF	CITATIONS
127	Analysis of the upconversion processes of Nd3+ ions in transparent YAG ceramics. Ceramics International, 2014, 40, 15951-15956.	4.8	13
128	Temperature response of the whispering gallery mode resonances from the green upconversion emission of an Er3+–Yb3+ co-doped microsphere. Laser Physics Letters, 2015, 12, 046003.	1.4	13
129	Temperature dependence of the whispering gallery modes obtained in a glass microsphere codoped with Er3+–Yb3+ ions. Sensors and Actuators A: Physical, 2015, 233, 422-426.	4.1	13
130	Slow magnetic relaxation mechanisms in erbium SIMs. Dalton Transactions, 2015, 44, 1264-1272.	3.3	13
131	Blue up-conversion emission of Yb3+-doped langbeinite salts. Optical Materials, 2016, 53, 190-194.	3.6	13
132	Upconversion emission of a novel glass ceramic containing Er 3+ , Yb 3+ :Sr 1â^'x Y x F 2+x nano-crystals. Journal of Luminescence, 2016, 172, 201-207.	3.1	13
133	Blue–green cooperative upconverted luminescence and radiative energy transfer in Yb 3+ -doped tungsten tellurite glass. Journal of Luminescence, 2016, 169, 233-237.	3.1	13
134	Luminescence properties of Pr3+ ion doped Mg-picromerite Tutton salt. Journal of Luminescence, 2017, 188, 148-153.	3.1	13
135	Synthesis and optical characterization of Er-doped bismuth titanate nanoparticles grown by sol–gel hydrothermal method. Ceramics International, 2017, 43, 3623-3630.	4.8	13
136	Structural, Vibrational, and Elastic Properties of Yttrium Orthoaluminate Nanoperovskite at High Pressures. Journal of Physical Chemistry C, 2017, 121, 15353-15367.	3.1	13
137	Downshifting maximization procedure applied to [Eu(bphen)(tta)3] at different concentrations applied to a photovoltaic device and covered with a hemispherical reflector. Sensors and Actuators A: Physical, 2018, 271, 60-65.	4.1	13
138	Upconversion in Detail: Multicolor Emission of Yb/Er/Tmâ€Đoped Nanoparticles under 800, 975, 1208, and 1532 nm Excitation Wavelengths. Particle and Particle Systems Characterization, 2020, 37, 2000068.	2.3	13
139	Excited-state dynamics in Yb3+-Ho3+-doped fluoroindate glasses. Journal of Applied Spectroscopy, 1995, 62, 865-871.	0.7	12
140	Optical amplification properties of Dy3+-doped Gd2SiO4, Lu2SiO5 and YAl3(BO3)4 single crystals. Applied Physics B: Lasers and Optics, 2011, 103, 597-602.	2.2	12
141	Site selective luminescence of Eu3+ ions in K2Mg(SO4)2â‹6H2O crystal. Optical Materials, 2015, 46, 339-344.	3.6	12
142	Synthesis, structural characterization and optical study of Dy 3+ -doped langbeinite salts. Journal of Luminescence, 2016, 177, 160-165.	3.1	12
143	Up-conversion photoluminescence of BaTiO3 doped with Er3+ under excitation at 1500 nm. Materials Research Bulletin, 2017, 86, 95-100.	5.2	12
144	1000ÂK optical ratiometric thermometer based on Er3+ luminescence in yttrium gallium garnet. Journal of Alloys and Compounds, 2021, 886, 161188.	5.5	12

INOCENCIO RAFAEL MARTIN

#	Article	IF	CITATIONS
145	High-pressure luminescence in Nd3+-doped MgO:LiNbO3. High Pressure Research, 2006, 26, 341-344.	1.2	11
146	Dielectric anomalies in Nd3+ doped Ba2NaNb5O15 laser crystal. Journal of Alloys and Compounds, 2008, 451, 198-200.	5.5	11
147	Role of the local structure and the energy trap centers in the quenching of luminescence of the Tb3+ ions in fluoroborate glasses: A high pressure study. Journal of Chemical Physics, 2010, 132, 114505.	3.0	11
148	Laser emission in Nd <sup>3+</sup> doped barium–titanium–silicate microspheres under continuous and chopped wave pumping in a non-coupled pumping scheme. Laser Physics, 2013, 23, 075801.	1.2	11
149	Photon avalanche upconversion in Ho3+-doped gallium nano-garnets. Optical Materials, 2015, 39, 16-20.	3.6	11
150	Portable IR dye laser optofluidic microresonator as a temperature and chemical sensor. Optics Express, 2016, 24, 14383.	3.4	11
151	Visible and NIR emitting Yb( <scp>iii</scp> ) and Er( <scp>iii</scp> ) complexes sensitized by β-diketonates and phenanthroline derivatives. RSC Advances, 2020, 10, 27815-27823.	3.6	11
152	Polymeric waveguides using oxidized porous silicon cladding for optical amplification. Optical Materials, 2009, 31, 1488-1491.	3.6	10
153	Nanocrystals distribution inside the writing lines in a glass matrix using Argon laser irradiation. Optics Express, 2010, 18, 582.	3.4	10
154	Energy transfer processes in Eu3+ doped nanocrystalline La2TeO6 phosphor. Journal of Luminescence, 2014, 145, 553-556.	3.1	10
155	Photoluminescence and energy transfer studies in Ce3+-Sm3+ co-doped phosphate glasses. Journal of Luminescence, 2022, 241, 118471.	3.1	10
156	Multifunctional cellulose fibers: Intense red upconversion under 1532Ânm excitation and temperature-sensing properties. Carbohydrate Polymers, 2022, 294, 119782.	10.2	10
157	Site distribution in Cr3+ and Cr3+-Tm3+-doped alkaline silicate glasses. Journal of Luminescence, 1997, 72-74, 446-448.	3.1	9
158	Desvitrification on an oxyfluoride glass doped with Tm3+ and Yb3+ ions under Ar laser irradiation. Journal of Luminescence, 2008, 128, 905-907.	3.1	9
159	Optical amplification by upconversion in Tm–Yb fluoroindate glass. Optical Materials, 2010, 32, 1349-1351.	3.6	9
160	Transfer and backtransfer processes in Yb3+–Er3+ codoped Strontium Barium Niobate glass-ceramics. Journal of Luminescence, 2011, 131, 2446-2450.	3.1	9
161	Stimulated emission in the red, green, and blue in a nanostructured glass ceramics. Journal of Applied Physics, 2011, 109, 043102-043102-6.	2.5	9
162	Study of the focusing effect of silica microspheres on the upconversion of Er3+–Yb3+ codoped glass ceramics. Journal of Alloys and Compounds, 2013, 576, 363-368.	5.5	9

#	Article	IF	CITATIONS
163	Effect of substitution of lutetium by gadolinium on emission characteristics of (Lu_xGd_1-x)_2SiO_5: Sm^3+ single crystals. Optical Materials Express, 2014, 4, 739.	3.0	9
164	A direct white-light-emitting coordination polymers with tunable green–white photoluminescence by variation of counterion. Inorganic Chemistry Communication, 2014, 39, 14-20.	3.9	9
165	Cathode and ion-luminescence of Eu:ZnO thin films prepared by reactive magnetron sputtering and plasma decomposition of non-volatile precursors. Journal of Luminescence, 2016, 178, 139-146.	3.1	9
166	Spectroscopic properties of Nd 3+ ions in YAP nano-perovskites. Journal of Luminescence, 2017, 188, 204-208.	3.1	9
167	Near-infrared and blue cooperative Yb3+ luminescence in Lu3Sc2Ga3O12 nano-garnets. Materials Research Bulletin, 2018, 101, 347-352.	5.2	9
168	Nanoperovskite doped with Yb3+ and Tm3+ ions used as an optical upconversion temperature sensor. Optical Materials, 2018, 83, 187-191.	3.6	9
169	Energy transfer, structural and luminescent properties of the color tunable phosphor Y2WO6:Sm3+. Journal of Alloys and Compounds, 2020, 835, 155381.	5.5	9
170	Energy transfer and up-conversion in Yb-Tm codoped fluorindate glasses. Radiation Effects and Defects in Solids, 1995, 135, 129-132.	1.2	8
171	Optical properties and site distribution of Cr3+ ions in alkali-disilicate glasses. Journal of Luminescence, 2004, 106, 77-90.	3.1	8
172	Energy transfer in Pr3+–Yb3+ codoped oxyfluoride glass ceramics. Optical Materials, 2007, 29, 1231-1235.	3.6	8
173	Optical amplification in Er3+-doped transparent Ba2NaNb5O15 single crystal at 850 nm. Journal of Applied Physics, 2009, 106, 113108.	2.5	8
174	Local devitrification on an oxyfluoride glass doped with Ho3+ ions under Argon laser irradiation. Optical Materials, 2009, 31, 1373-1375.	3.6	8
175	Optical gain in Er3+-doped transparent LuVO4 crystal at 850nm. Optical Materials, 2010, 32, 475-478.	3.6	8
176	Synthesis, structural modelling and luminescence of a novel erbium(III) complex with 2,4-nonanedione and 2,2′-bipyridine ligands for chitosan matrices doping. Optical Materials, 2015, 41, 139-142.	3.6	8
177	Regular oscillations and random motion of glass microspheres levitated by a single optical beam in air. Optics Express, 2016, 24, 2850.	3.4	8
178	Alternative and fully experimental procedure for characterizing down-shifters placed on photovoltaic devices. Solar Energy Materials and Solar Cells, 2018, 185, 312-317.	6.2	8
179	Fluorescence intensity ratio and whispering gallery mode techniques in optical temperature sensors: comparative study. Optical Materials Express, 2019, 9, 4126.	3.0	8
180	Site selective spectroscopy of Eu <sup>3+</sup> and Eu <sup>3+</sup> -Ho <sup>3+</sup> doped glasses. Radiation Effects and Defects in Solids, 1995, 135, 105-108.	1.2	7

#	Article	IF	CITATIONS
181	Kinetics of transfer and backtransfer in Yb3+-Er3+ codoped fluoroindate glasses. Journal of Luminescence, 1997, 72-74, 954-955.	3.1	7
182	Optical Properties of Rare Earth Doped Transparent Oxyfluoride Glass Ceramics. Radiation Effects and Defects in Solids, 2003, 158, 457-462.	1.2	7
183	Optical properties of Eu3+ ions in malonate crystals to monitor a structural phase transition. Optical Materials, 2004, 25, 223-229.	3.6	7
184	Room temperature infrared-laser-induced upconversion in Nd3+ doped Ta2O5 waveguides. Chemical Physics Letters, 2006, 421, 198-204.	2.6	7
185	Optical study of the effect of the impurity content on the ferroelectric properties of Er3+ doped SBN glass-ceramic samples. Journal of Applied Physics, 2011, 110, .	2.5	7
186	Local characterization of rare-earth-doped single microspheres by combined microtransmission and microphotoluminescence techniques. Journal of the Optical Society of America B: Optical Physics, 2012, 29, 3293.	2.1	7
187	Investigation on Crystallization and Optical Properties of <scp><scp>Ca</scp></scp> <sub>1<i>â°x</i></sub> <scp><scp>La</scp></scp> <sub><i>x</i></sub> <scp><sc Glassâ€Ceramics. Journal of the American Ceramic Society, 2014, 97, 782-788.</sc </scp>	:p> <b>₿</b> &scp>	• <b scp> <sub< td=""></sub<>
188	Spontaneous and stimulated emission in Sm3+-doped YAl3(BO3)4 single crystal. Journal of Luminescence, 2015, 167, 163-166.	3.1	7
189	Adaptive WHTS-Assisted SDMA-OFDM Scheme for Fair Resource Allocation in Multi-User Visible Light Communications. Journal of Optical Communications and Networking, 2016, 8, 427.	4.8	7
190	Timing synchronization for OFDM-based visible light communication system. , 2016, , .		7
191	A compact and portable optofluidic device for detection of liquid properties and label-free sensing. Journal Physics D: Applied Physics, 2017, 50, 215103.	2.8	7
192	Laser Refrigeration by an Ytterbiumâ€Đoped NaYF <sub>4</sub> Microspinner. Small, 2021, 17, e2103122.	10.0	7
193	Cr3+–Tm3+ energy transfer in alkali silicate glasses. Journal of Alloys and Compounds, 2001, 323-324, 759-762.	5.5	6
194	Spectroscopic Monitoring of the Eu 3+ Ion Local Structure in the Pressure Induced Amorphization Of EuZrF 7 Polycrystal. High Pressure Research, 2002, 22, 111-114.	1.2	6
195	Upconversion emission in Er3+-doped lead niobium germanate thin-film glasses produced by pulsed laser deposition. Applied Physics A: Materials Science and Processing, 2008, 93, 621-625.	2.3	6
196	Localized desvitrifiation in Er3+-doped strontium barium niobate glass by laser irradiation. Applied Physics A: Materials Science and Processing, 2008, 93, 977-981.	2.3	6
197	Optical amplification in Er3+-doped fluoroindate glass at 840nm and 1550nm. Optical Materials, 2009, 31, 1370-1372.	3.6	6
198	Nanocrystal formation using laser irradiation on Nd3+ doped barium titanium silicate glasses. Journal of Alloys and Compounds, 2013, 553, 35-39.	5.5	6

#	Article	IF	CITATIONS
199	Synthesis, luminescence, and electrical properties of Na6Mg(SO4)4:xEu vanthoffite ceramics as electrode materials for sodium ion batteries. Materials Science and Engineering B: Solid-State Materials for Advanced Technology, 2019, 247, 114384.	3.5	6
200	Behavior of Yb <sup>3+</sup> and Er <sup>3+</sup> during Heat Treatment in Oxyfluoride Class Ceramics. Journal of Nanomaterials, 2014, 2014, 1-10.	2.7	5
201	High pressure sensitivity of anti-Stokes fluorescence in Nd3+ doped yttrium orthoaluminate nano-perovskites. Journal of Luminescence, 2018, 196, 20-24.	3.1	5
202	Holmium doped fiber thermal sensing based on an optofluidic Fabry-Perot microresonator. Journal of Luminescence, 2019, 206, 492-497.	3.1	5
203	Highly luminescent mixed-ligand bimetallic lanthanoid( <scp>iii</scp> ) complexes for photovoltaic applications. Dalton Transactions, 2022, 51, 3146-3158.	3.3	5
204	Optical properties of Eu3+ and Ho3+ in fluoride glasses. Journal of Applied Spectroscopy, 1995, 62, 766-770.	0.7	4
205	Local crystallization in an oxyfluoride glass doped with Er3+ ions using a continuous argon laser. Applied Physics A: Materials Science and Processing, 2008, 93, 983-986.	2.3	4
206	Structural changes induced on strontium barium niobate glass byÂfemtosecond laser irradiation. Applied Physics A: Materials Science and Processing, 2010, 98, 879-884.	2.3	4
207	Crystallization effect on Tm3+–Yb3+ codoped SBN glass ceramics. Optical Materials, 2010, 32, 1385-1388.	3.6	4
208	Enhanced energy upconversion and super-resolved focused spot generation in Tm^3+-Yb^3+ codoped glass using silica microspheres. Journal of the Optical Society of America B: Optical Physics, 2013, 30, 1392.	2.1	4
209	Multi-User Visible Light Communications. , 2014, , .		4
210	Glass heating through submicron spots produced with silica microspheres. Journal of Luminescence, 2016, 180, 8-13.	3.1	4
211	Enhanced green fluorescent protein in optofluidic Fabry-Perot microcavity to detect laser induced temperature changes in a bacterial culture. Applied Physics Letters, 2017, 111, .	3.3	4
212	X-ray nanoimaging of Nd^3+ optically active ions embedded in Sr_05Ba_05Nb_2O_6 nanocrystals. Optical Materials Express, 2017, 7, 2424.	3.0	4
213	Near infrared and upconversion luminescence of Tm3+-Yb3+codoped CdF2 single crystals. Journal of Luminescence, 2020, 228, 117594.	3.1	4
214	Temperature Sensing with Nd3+ Doped YAS Laser Microresonators. Applied Sciences (Switzerland), 2021, 11, 1117.	2.5	4
215	Temperature sensor based on luminescence intensity ratio or whispering gallery modes in phosphate glass co-doped with Pr3+ and Yb3+. Optics and Laser Technology, 2022, 149, 107893.	4.6	4

Porous silicon-based notch filters and waveguides. , 2005, , .

#	Article	IF	CITATIONS
217	Analysis of the optical properties of Er3+-doped strontium barium niobate nanocrystals using time-resolved laser spectroscopy. Applied Physics A: Materials Science and Processing, 2010, 99, 771-776.	2.3	3
218	Second harmonic generation in Er3+–Yb3+:YBO3. Materials Letters, 2010, 64, 650-653.	2.6	3
219	Formation of Nd3+ doped Strontium Barium Niobate nanocrystals by two different methods. Optical Materials, 2010, 32, 1389-1392.	3.6	3
220	Nanocrystals formation on Ho3+ doped strontium barium niobate glass. Journal of Luminescence, 2011, 131, 657-661.	3.1	3
221	Investigation of spectroscopic properties and energy transfer between Ce and Dy in (Lu0.2Gd0.8â^'xâ^'yCexDyy)2SiO5 single crystals. Journal of Luminescence, 2015, 166, 304-312.	3.1	3
222	Pressure- and temperature-induced structural phase transitions in fluoride matrices monitoring by Eu3+luminescence. High Pressure Research, 2006, 26, 411-414.	1.2	2
223	Optical gain in dye-doped polymer waveguides using oxidized porous silicon cladding. , 2007, , .		2
224	Optical properties of Nd3+-doped Tutton salts crystals. Journal of Luminescence, 2017, 192, 136-140.	3.1	2
225	Europium and potassium co-doped strontium metaborate single crystals grown by the Czochralski method. Journal of Crystal Growth, 2017, 457, 107-111.	1.5	2
226	Synthesis, structural characterization and luminescence properties of new Na0.3-x NdxAl0.3Si0.7O2+l̂´ (O–0.1) ceramics for optical applications. Journal of Materials Research and Technology, 2021, 13, 1181-1190.	5.8	2
227	Improving the sensitivity of WGM pressure sensors with oxyfluoride glass microspheres. Journal of Luminescence, 2021, 238, 118249.	3.1	2
228	Analysis of down conversion and back-transfer processes in Pr3+-Yb3+ co-doped phosphate glasses. Optical Materials, 2022, 131, 112604.	3.6	2
229	Growth of Nanocrystals in a Nd <sup>3+</sup> –Yb <sup>3+</sup> Codoped Oxyfluoride Glass by Laser Irradiation. Journal of Nanoscience and Nanotechnology, 2009, 9, 3771-3774.	0.9	1
230	Control of the local devitrification on oxyfluoride glass doped with Er3+ ions under diode laser irradiation. Journal of Applied Physics, 2010, 108, 103103.	2.5	1
231	Optical gain by upconversion in Tm–Yb oxyfluoride glass ceramic. Applied Physics B: Lasers and Optics, 2011, 104, 237-240.	2.2	1
232	Up-conversion processes in Ln(III)-doped luminescent materials for photovoltaics and photocatalysis. , 2018, , 291-333.		1
233	Energy Transfer Studies in Tb3+-Yb3+ Co-Doped Phosphate Glasses. Materials, 2021, 14, 6782.	2.9	1
234	Optical spectroscopy of Cr3+ and Cr3+-Tm3+ in alkaline silicate glasses. Journal of Applied Spectroscopy, 1995, 62, 895-899.	0.7	0

#	Article	IF	CITATIONS
235	Room temperature photon avalanche upconversion in Ho3+doped fluoroindate glasses under excitation at 749 nm. , 2003, 4829, 141.		0
236	Optical properties of Eu3+in malonate crystals to monitor a structural phase transition. , 2003, , .		0
237	Optical gain in oxidized porous silicon waveguides impregnated with a laser dye. Physica Status Solidi C: Current Topics in Solid State Physics, 2007, 4, 2145-2149.	0.8	0
238	Waveguiding, absorption and emission properties of dye-impregnated oxidized porous silicon. Physica Status Solidi (A) Applications and Materials Science, 2007, 204, 1502-1506.	1.8	0
239	Upconversion emission in rare earth doped materials under near infrared excitation using silica microspheres as focusing lenses. , 2013, , .		0
240	Clustering of Aerosols in a Single Potential-well Trap. , 2013, , .		0
241	Possible non-centrosymmetric structure of vaterite type yttrium orthoborate. Acta Crystallographica Section A: Foundations and Advances, 2008, 64, C467-C468	0.3	Ο